



Microscopic mechanism of martensitic stabilization in shape-memory alloys: Atomic-level processes

Junkai Deng,^{1,2} Xiangdong Ding,^{1,3,*} Turab Lookman,³ Tetsuro Suzuki,² Kazuhiro Otsuka,² Jun Sun,¹ Avadh Saxena,³ and Xiaobing Ren^{2,†}

¹*Multi-disciplinary Materials Research Center, Frontier Institute of Science and Technology and State Key Laboratory for Mechanical Behavior of Materials, Xi'an Jiaotong University, Xi'an 710049, China*

²*Ferroc Physics Group, National Institute for Materials Science, Tsukuba, 305-0047 Ibaraki, Japan*

³*Theoretical Division, Los Alamos National Laboratory, Los Alamos, New Mexico 87545, USA*

(Received 8 February 2010; revised manuscript received 15 April 2010; published 17 June 2010)

Aging in martensite, which is accompanied by a gradual change in physical properties, has been observed in most shape-memory alloys for more than half a century. However, its microscopic mechanism has remained controversial due to a lack of experiments that can probe the atomic-level processes. By using a method which combines molecular-dynamics and Monte Carlo simulations, we clarify the atomic mechanism for one of the well-observed martensitic aging effects, martensitic stabilization. We successfully reproduce the observed effects using our method. Quantitative analysis of the atomic configurations during aging reveals that martensite stabilization is not associated with a change in the average martensite structure. It involves instead a gradual change in the short-range order of point defects so that the defect short-range order tends to adopt the same “symmetry” as the crystal symmetry of the host martensite lattice. Our simulation results are consistent with the symmetry-conforming short-range order model [X. Ren and K. Otsuka, *Nature (London)* **389**, 579 (1997)].

DOI: [10.1103/PhysRevB.81.220101](https://doi.org/10.1103/PhysRevB.81.220101)

PACS number(s): 61.72.sh, 61.72.Bb, 64.60.De, 66.30.J–

Shape-memory alloys (SMAs) are widely known as functional materials due to their unique shape-memory and superelastic properties. However, a majority of SMAs, such as Au-Cd, Au-Cu-Zn, Cu-Zn-Al, Cu-Al-Ni, Ti-Ni-Hf, and Ni-Mn-Ga, exhibit martensite aging effects,^{1–7} which lead to a gradual change in physical properties with aging. As aging effects, in general, are undesirable in applications of shape-memory alloys,⁸ the problem is of considerable interest and has been actively pursued in order to understand its origin.

Martensitic stabilization, as one of the typical martensite aging effects, refers to the phenomenon in which martensite becomes more stable with aging so that the reverse-transformation-finish temperature (A_f) increases with aging time. This time-dependent behavior is critical to the reliability of devices using SMA as it is desirable to have a reproducible and stable transformation temperature. Therefore, understanding the origin of martensitic stabilization is of both fundamental and practical importance.

The origin of martensitic stabilization in alloys undergoing a martensitic transformation has been a long-standing puzzle. Experiments on stable or equilibrium martensites, such as Au-Cd (Ref. 2) and Au-Cu-Zn,^{3,9} have proved that martensitic stabilization develops even without any detectable change in average martensite structure. This seemingly perplexing result is, in fact, very natural as the average structure of the equilibrium or stable phase is not expected to depend on time (aging). The outstanding puzzle is why and how a phase in thermodynamic equilibrium (martensite) can change its transformation behavior without leading to any average structure change.

Over the last several decades, there have been numerous studies aiming at clarifying the origin of this challenging problem and several microscopic models have been proposed, such as the long-range order [LRO (Ref. 4)] and the short-range order [SRO (Refs. 10 and 11)] models. However,

there has been no consensus due to the lack of experiment that probes the atomic processes at work during aging in martensite. Hence, the mechanism of martensitic stabilization remains controversial.

In this Rapid Communication, by means of a combined molecular-dynamics (MD) and the Monte Carlo (MC) simulation technique, which can deal with both the short-time-scale martensitic transformation and long-time-scale aging problem, we successfully reproduced the experimentally observed martensitic stabilization phenomenon, as well as clarified its microscopic mechanism at atomic scale. From the atomic redistribution during aging, we found that martensitic stabilization is caused by a gradual change in the “symmetry” of SRO of point defects, rather than a change in the long-range order or average structure. Our simulation results support the symmetry-conforming SRO (SC-SRO) model¹¹ for martensitic stabilization.

Martensitic stabilization is associated with an increase in the reverse-transformation-finish temperature (A_f) with time due to aging in martensite. To capture the key features of this phenomenon, one first needs to reproduce the whole martensitic transformation and reverse transformation processes, and then simulate the aging process itself in martensite. As martensitic transformation is a very fast diffusionless process, it is amenable to study by MD simulations, which provide a powerful means to investigate martensitic (or reverse) transformations. However, the maximum time that MD simulations can reach is too short (up to microsecond reported so far) to investigate the aging process (within the order of seconds to years) in a real martensitic system. On the other hand, the classical MC method is more suitable to investigate the long-time aging process involving atomic diffusion, but it cannot give us the kinetics of the martensitic transformation.

In this work, we combined MD simulations with the classical MC method to reproduce the phenomenon of martensi-

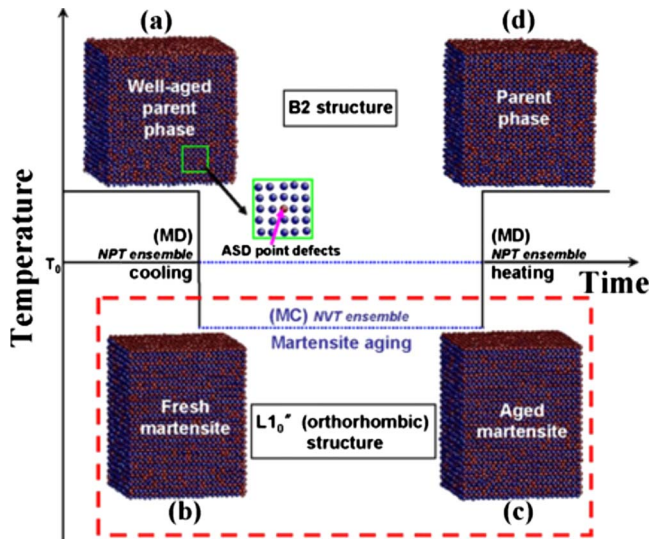


FIG. 1. (Color online) Schematic illustration of the present simulations: (a) Well-aged parent phase with B2 structure is obtained by the combination of MD and MC methods, which contains 5 at. % ASDs. (b) Martensitic phase transformation takes place during the cooling process by MD simulation, the fresh martensite with $L1_0''$ (orthorhombic) structure is formed. (c) Aging for different MC steps to produce a group of different-time-aged martensite samples. (d) The reverse martensitic phase transformation occurs during heating process by using MD and martensitic stabilization behavior is investigated.

tic stabilization from the atomic level. Figure 1 depicts a schematic illustration of our simulation processes by this approach. First, the MD method was used to obtain a stable parent phase at a normalized temperature (0.54) above A_f . The corresponding atomic configurations and lattice parameters were then transferred to the MC model to simulate atomic-diffusion processes and obtain a well-aged parent phase [Fig. 1(a)]. Second, the atomic information of the well-aged, equilibrium parent phase was again introduced to the MD simulation to cool the ensemble down to a normalized temperature (0.34) below the martensitic transformation-finish temperature (M_f) to obtain the fresh martensite [Fig. 1(b)]. Only one perfect single-domain martensite was generated. The average atomic configurations of fresh martensite were then introduced into the MC model, and aged for different MC steps to obtain a group of martensites with different aging times [Fig. 1(c)]. Finally, the atomic configurations of the aged martensite were studied by MD, and the ensemble was heated up to the parent phase [Fig. 1(d)]. In this way, we could finally detect the change in A_f with the time of aging in the martensite. In order to clarify the corresponding microscopic mechanism, the atomic distributions during aging were also recorded and analyzed.

As it is experimentally known that the martensite aging effects are strongly dependent on the point defects,¹² we established a binary alloy $A_{55}B_{45}$ with B2 structure as our model material (shown in Fig. 1), in which 5 at. % of A atoms were introduced in the β sublattice (occupied by B atoms) as the antisite point defects (ASDs). The present MD method is based on the Parinello-Rahman scheme¹³ with a simple 8-4 Lennard-Jones potential¹⁴ (instead of the standard

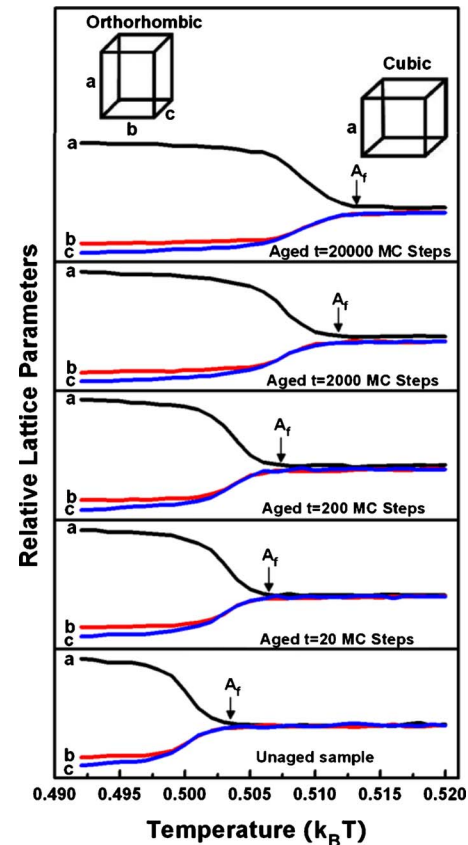


FIG. 2. (Color online) Martensitic stabilization behavior: reverse martensitic transformations from $L1_0''$ (orthorhombic) structure to B2 structure take place during the heating process by MD simulation [corresponding to the processes shown in Figs. 1(c) to 1(d)] and the A_f temperature increases with aging time.

12-6 Lennard-Jones potential), which has been successfully used to simulate a generic martensitic transformation (B2 to $L1_0''$, which is an $L1_0$ -based orthorhombic structure).^{14,15} The initial MD model is built in a cubic box with B2 structure containing $48 \times 48 \times 48$ unit cells, isothermal-isobaric ensemble and periodic boundary conditions in three dimensions were used. As there is no change in average structure during the aging process, canonical ensemble was used during the present MC simulation, which is based on the Metropolis algorithm.¹⁶ It should be noted that our MC step means one attempt of exchanging two neighboring atoms, thus reflecting the atomic-diffusion process of aging. Therefore, MC steps can be used as a measure of aging time. The normalized temperature and lattice constants were used in both MD and MC simulations.

By means of the above approach, we studied the effects of aging in martensite on the reverse-transformation temperature. For the ensemble which are aged in martensite for different times (0, 20, 200, 2000, 20 000 MC steps, respectively), Fig. 2 gives the corresponding change in lattice constants during the heating process (as a monitor of the reverse transformation). Furthermore, the change in reverse-transformation-finish temperature (A_f) with MC steps is shown in Fig. 3(a). From these figures, we can clearly see that the reverse-transformation-finish temperature A_f from $L1_0''$ (orthorhombic structure) to B2 structure increases with

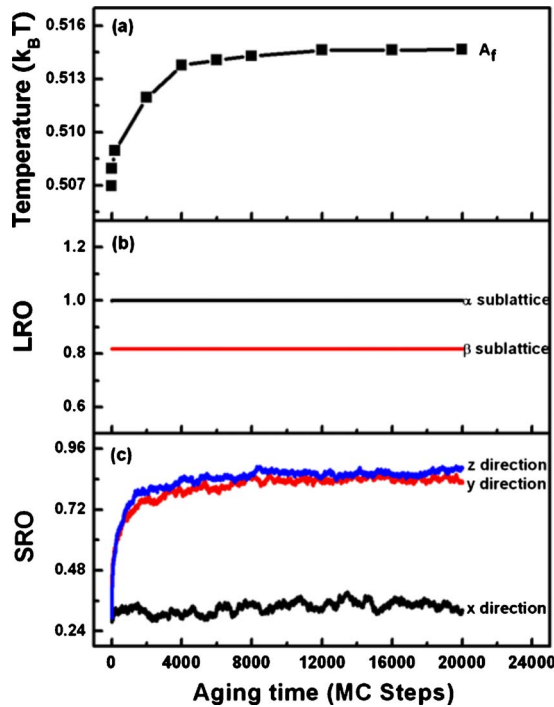


FIG. 3. (Color online) Variation in (a) A_f temperature, (b) LRO, and (c) SRO parameters during aging in martensite [corresponding to the processes shown in Figs. 1(b) to 1(c)].

the increase in time of aging in martensite and eventually saturates at long aging time, which is consistent with experimental results.^{2,3} Thus the present method successfully reproduces the phenomenon of martensitic stabilization. In addition, we found that atomic configurations vary with MC steps; this further confirms that the martensitic stabilization is associated with the diffusion of atoms (or defects).

As our system is an essentially ordered one, the migration or diffusion of the atoms or defects will have two possible consequences: (1) changing the LRO, i.e., the average structure, and (2) changing SRO while keeping the same long-range order or average structure. The variation in LRO or SRO usually causes the change in physical properties in ordered crystal.¹⁷ In the following, we shall calculate the change in LRO and SRO during the martensitic aging process [corresponding to Figs. 1(b) to 1(c)] and explore which process is responsible for the change in reverse-transformation-finish temperature A_f .

Figure 3(b) shows the change in LRO with the aging in martensite. Here, the LRO is defined as follows:¹⁸

$$L_\alpha = \frac{r_\alpha - x_A}{1 - x_A}; \quad L_\beta = \frac{r_\beta - x_B}{1 - x_B}, \quad (1)$$

where L_α and L_β are the LRO parameters of α sublattice and β sublattice, respectively; r_α is the fraction of α sublattice occupied by the appropriate atoms (A atoms in α sublattice); r_β is the fraction of β sublattice occupied by the appropriate atoms (B atoms in β sublattice); x_A or x_B is the mole fraction of atom A or B in the alloy, respectively. According to the above definition, for the present $A_{55}B_{45}$ model material, the initial value of L_α and L_β are 1 and 0.818, respectively.

From Fig. 3(b), it is clear that there is no change in LRO

during the aging process in martensite in either α or β sublattices. This indicates that there is no change in average structure during the aging process, which is also consistent with available experimental observations on Au-Cd (Ref. 2) and Au-Cu-Zn (Ref. 9) martensite. The fact that $L_\alpha=1$ and does not change during aging also indicates that the net exchange of atoms (or defects) only takes place within the same sublattice (β sublattice) of the ordered martensite, not between α and β sublattices.

Following Cowley¹⁹ we define SRO, short-range order, of point defects in β sublattice as follows:

$$s_{lmn} = 1 - \frac{P_i^D | j^D}{x_D}, \quad (2)$$

where lmn are the coordinates of the interatomic vector between sites i and j ; the conditional probability $P_i^D | j^D$ is the probability to find an ASD at site i if there is an ASD at site j ; x_D is the atomic fraction of ASDs. From this definition, apparently SRO in a crystal lattice should be direction dependent.

Figure 3(c) shows the change in SRO of nearest sites along [100], [010], and [001] of β sublattice with the aging process in martensite. It is clear that the defect SRO changes during the aging process. For the fresh martensite, i.e., before aging, the defect SRO along [100], [010], and [001] directions are almost the same. However, with the increase in aging in martensite, the defect SRO along the above three directions gradually become different, and, the values of defect SRO in the above three directions tend to saturate finally.

Interestingly, if we compare the change in A_f temperature with aging time in martensite with that of defect LRO and SRO [Figs. 3(a)–3(c)], we can find that the change in A_f temperature with aging is synchronous with that of defect SRO and does not correlate with that of defect LRO. It indicates that the origin of martensitic stabilization is closely related to the change in defect SRO during the aging in martensite and is not associated with the change in LRO, i.e., the change in the average crystal structure.

Based on the above results, we are able to evaluate the previous models for martensitic stabilization from the atomic level. Apparently, the absence of the LRO change in the present simulation indicates that the model⁴ which supposes (or results in) a change in the long-range order structure is excluded. It is to be noted that some Cu-based metastable martensites have an innate tendency to decompose into their equilibrium products so that the martensite aging effect is accompanied by a LRO change.⁴ However, it is clearly an extrinsic effect. Stable martensites like Au-Cd and Au-Cu-Zn do not show a change in LRO.^{2,9}

On the other hand, the significant change in SRO during aging in our simulations indicates that the reported short-range ordering models^{10,11} are the potential candidates for understanding the nature of martensitic stabilization. However, some SRO models¹⁰ require the change in pair (bond) probability of nearest neighbors and net atom/defect exchange between sublattices for ordered alloy. Such short-range ordering will inevitably change the LRO of the ordered

alloy, and contradict our simulation results, and also inconsistent with the experimental observations on nondecomposing martensite.²

The other SRO model for the martensitic stabilization is the SC-SRO principle proposed by Ren and Otsuka.^{11,20} It states that the most stable state for a crystal with point defects is a state in which the symmetry of defect short-range order in equilibrium conforms to the symmetry of the host crystal lattice. According to this model, to minimize the total energy of the system, the defect SRO in parent phase should possess the cubic symmetry, which indicates that the defect SRO along [100], [010], and [001] directions should be the same. Although the SRO symmetries of point defects can be inherited in fresh martensite state through martensitic transformation, the equilibrium symmetry of SRO in martensite should present the same symmetry of martensite (orthorhombic symmetry), and the defect SRO along [100], [010], and [001] directions is no longer the same.

Interestingly, our simulation results are quite consistent with the prediction of the SC-SRO model. Figure 4 shows the changes in point-defect SRO with the processes shown in Figs. 1(a)–1(c). For clarity of illustration, we only show the symmetry of point defects in two dimension which is a projection of (010) plane. As depicted in this figure, although the distribution of point defects is random as a whole, the SRO values of point defects reveal a symmetry property. As shown in Fig. 4(a), the SRO of point defects in the equilibrium parent phase possesses cubic symmetry since the values of defect SRO along [100] and [001] directions are essentially the same. After martensitic transformation, the SRO of point defects in fresh martensite still keeps the same symmetry as that of the parent phase [Fig. 4(b)]. However, after aging in martensite, the SRO of point defects becomes different along [100] and [001] directions [Fig. 4(c)]. It indicates that the symmetry of SRO in aged martensite becomes lower and tends to follow the crystal symmetry of martensite. Therefore, our results support the SC-SRO model as the most reasonable model for martensitic stabilization.

Finally, we note that models based on twin boundary pinning effect also exist,²¹ but our results suggest that the change in SRO symmetry during aging is the most fundamental process. This is consistent with the experimental find-

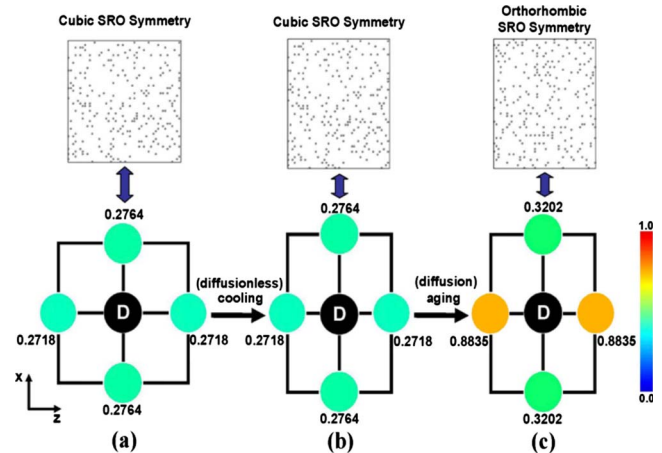


FIG. 4. (Color online) Changes in SRO of point defects during the processes shown in Figs. 1(a)–1(c). For simplicity, the (010) plane of our model is shown: (a) defect symmetry around a known defect in the parent phase; note the essentially equal probability for the presence of a defect at the neighboring sites. (b) Defect symmetry around a known defect in fresh $L1_0$ martensite. (c) Defect symmetry around a known defect in well-aged $L1_0$ martensite; note the change in defect probability.

ing that aging effect exists even in single-domain martensite (i.e., without twin boundaries).²²

In conclusion, we successfully reproduced the martensitic stabilization from the atomic level by combining of MD and MC methods. Microscopic analysis revealed that the origin of martensitic stabilization is not related to the change in long-range order; but is instead due to a change in short-range order of point defects within the same sublattice. Defect short-range order tends to adopt the same “symmetry” as that of the crystal; this supports the symmetry-conforming short-range order principle of point defects.

We thank Y. Wang, Z. Zhang, and S. Li for stimulating discussions and useful suggestions. This work was supported by NSFC (Grants No. 50771079 and No. 50720145101), the 973 Program of China (Grant No. 2010CB631003), and 111 Project as well as the support from the U.S. DOE at LANL (Grant No. DE-AC52-06NA25396).

*Corresponding author. dingxd@mail.xjtu.edu.cn

†Corresponding author. ren.xiaobing@nims.go.jp

¹A. Ölander, *J. Am. Chem. Soc.* **54**, 3819 (1932).

²Y. Murakami *et al.*, *Mater. Sci. Eng., A* **237**, 87 (1997).

³T. Tadaki *et al.*, *Mater. Trans., JIM* **31**, 941 (1990).

⁴A. A. Arab and M. Ahlers, *Acta Metall.* **36**, 2627 (1988).

⁵H. Sakamoto *et al.*, *Scr. Metall.* **11**, 607 (1977).

⁶R. Santamarta *et al.*, *Scr. Mater.* **41**, 867 (1999).

⁷C. Seguí *et al.*, *Scr. Mater.* **53**, 315 (2005).

⁸S. Miyazaki and K. Otsuka, in *Shape Memory Alloys*, edited by H. Funakubo (Gordon and Breach, New York, 1987), p. 116.

⁹T. Ohba *et al.*, *J. Phys. IV* **05**, C8-1083 (1995).

¹⁰K. Marukawa and K. Tsuchiya, *Scr. Metall. Mater.* **32**, 77 (1995); M. Ahlers *et al.*, *Scr. Metall.* **12**, 1075 (1978); T. Suzuki *et al.*, *J. Phys. IV* **05**, C8-1065 (1995).

¹¹X. Ren and K. Otsuka, *Nature (London)* **389**, 579 (1997).

¹²K. Otsuka *et al.*, *Mater. Sci. Eng., A* **273-275**, 558 (1999).

¹³M. Parrinello and A. Rahman, *J. Appl. Phys.* **52**, 7182 (1981).

¹⁴T. Suzuki and M. Shimono, *J. Phys. IV* **112**, 129 (2003).

¹⁵X. Ding, T. Suzuki, X. Ren, J. Sun, and K. Otsuka, *Phys. Rev. B* **74**, 104111 (2006); X. Ding *et al.*, *Mater. Sci. Eng., A* **438-440**, 113 (2006).

¹⁶N. Metropolis *et al.*, *J. Chem. Phys.* **21**, 1087 (1953).

¹⁷T. Castán and A. Planes, *Phys. Rev. B* **38**, 7959 (1988).

¹⁸W. L. Bragg and E. J. Williams, *Proc. R. Soc. London, Ser. A* **145**, 699 (1934).

¹⁹J. M. Cowley, *Phys. Rev.* **77**, 669 (1950).

²⁰X. Ren and K. Otsuka, *Phys. Rev. Lett.* **85**, 1016 (2000).

²¹J. Janssen *et al.*, *J. Phys.* **43**, C4-715 (1982).

²²Y. Murakami *et al.*, *J. Phys. IV* **05**, C8-1071 (1995).